Origin of zero-bias conductance peaks in high-T_c superconductors

Satoshi Kashiwaya
Electrotechnical Laboratory, Tsukuba, Ibaraki 305, Japan

Yukio Tanaka
Department of Physics, Niigata University, Igarashi, Niigata 950-21, Japan

Masao Koyanagi, Hiroshi Takashima, and Koji Kajimura
Electrotechnical Laboratory, Tsukuba, Ibaraki 305, Japan
(Received 24 June 1994)

A wide variety of experimental conductance spectra in high-T_c superconductors can be explained by a theory of proximity-electron-tunneling spectroscopy (PETS) for d-wave superconductors. From a solution of the Bogoliubov–de Gennes equation, the conductance spectra of the PETS are proved to show gap or zero-bias peak structures depending on the axis orientation of the superconductor. The features of the calculated spectra are consistent with the experimental results of $YBa_2Cu_3O_{7-\delta}$ observed by low-temperature scanning tunneling spectroscopy.

The symmetries of the pair potentials in high-T_c superconductors give important information to elucidate the mechanism of superconductivity in these materials. Many tunneling experiments have been devoted to this purpose, and a wide variety of conductance spectra is reported. For example, the conductance spectra with a flat bottom, which seems to indicate s-wave symmetry, are rarely observed.[1] On the other hand, many tunneling junctions showed zero-bias conductance peaks (ZBCP's).[2] Since these features of spectra cannot be explained by the tunneling theory of conventional superconductors, a new model is required to understand the tunneling effects of high-T_c superconductors. A recent report by Hu discussed the bound states in a normal metal (N) overlayer placed on a d-wave superconductor (S), concluding that midgap states were formed just at the Fermi level in N when S has d_{xy}-wave symmetry.[3] His results proposed a possibility to analyze the spectra in high-T_c superconductors by the proximity effect.

In this paper, we report the observation of the surface electronic states of $YBa_2Cu_3O_{7-\delta}$ (YBCO) films by low-temperature scanning tunneling microscopy and spectroscopy (LT-STM/S). The tunneling spectra showed gap and ZBCP in wide surface area of (100)-oriented films. The tunneling spectra are analyzed by the proximity-electron-tunneling spectroscopy (PETS) using the Bogoliubov-de Gennes equation. When S has $d_{x^2-y^2}$-wave symmetry with misorientation of the a axis relative to the normal vector of the N-S interface, the conductance spectrum of PETS is proved to show a ZBCP reflecting the formation of midgap states. It is revealed that many features of spectra observed on $YBa_2Cu_3O_{7-\delta}$ (YBCO) films are consistent with those of PETS of d-wave superconductors.

The advantages of tunneling spectroscopy by STM/S are that it has a capability of spectroscopy without spatial averaging and that we can check the morphology just at the same surface as that observed by spectroscopy. We measured many sputtered YBCO thin films with a-axis or c-axis orientations at 4.2 K. The films were mounted in a STM unit soon after they were taken out from the sputtering chamber to air. Mechanically ground Pt wires were used for a STM tip. The details of our system and sample preparation were described elsewhere.[4,5] The STM topographies were taken at high bias condition (≈ 1 V), because the STM servomotion was stable at this bias level. On the other hand, the spectra were taken at low bias (≈ 30 mV) to observe clearly the structure near the Fermi level. The topographies showed clear monolayer steps in the case of c-axis films, while in the case of a-axis films, amorphouslike corrugations with their heights from 1 to 10 nm were observed. The orientation of the axis at the topmost surface was not clear for a-axis films, because of their topographic corrugations. After the STM observation, the electronic states of the same surfaces were measured by spectroscopy mode. In the case of the c-axis film, gap structures were observed in most areas, and ZBCP's were observed only in a small area. In the case of the a-axis film, both ZBCP's and gap structures were observed. The ratio of areas showing each feature depended on samples. The maximum ratio of the area showing the ZBCP reached to nearly 70% of the scanning area of STM/S of about $0.1\times 0.1\ \mu m^2$. In such films, similar ZBCP's were observed continuously during a line scan of 10 nm. The correlation of the appearance of ZBCP with axis orientation is consistent with other reports,[6] which means that we are microscopically observing the same phenomena as other thin-film experiments. When a magnetic field (≈ 4 T, perpendicular to the surface) was applied, the ZBCP's responded to the applied field. Some of them split into two peaks or broadened. Typical conductance spectra of ZBCP without and with the magnetic field are shown in Fig. 1.

Next, the conductance spectra are analyzed by a simple N_1-I-N_2-S system in the clean limit. A step-function pair potential $\Theta(x)\Delta(\mathbf{k})$ is assumed, where $\Theta(x)$, $\mathbf{k}$ and $\Delta(\mathbf{k})$ are the step function, the relative wave vector of the Cooper pair, and the pair potential for an anisotropic su-

0163-1829/95/51(2)/1350(4)/$06.00

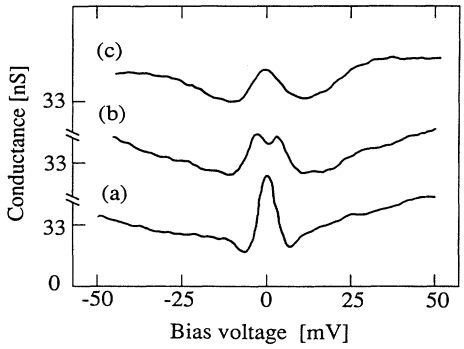

FIG. 1. Experimental spectra of a YBCO (100) film with the bias voltage of 30 mV and the current of 1 nA at 4.2 K: (a) typical spectrum showing the ZBCP in the absence of magnetic field; (b) and (c) typical spectra in the magnetic field of 4 T. The spectra of (b) and (c) were obtained at different surface points.

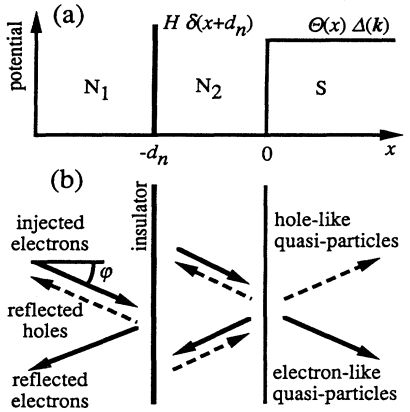

FIG. 2. Potential model of PETS. The insulator is described by a δ function whose amplitude is H, and the thickness of N_2 is d_n. (b) Trajectory of quasiparticles in PETS.

perconductor, respectively (Fig. 2). The Fermi wave number k_F and electron mass m in each region are assumed to be equal. Suppose electrons with energy E is injected from the left side with an angle φ. The injected electrons are transmitted to S as electronlike and holelike quasiparticles whose wave vectors are $\mathbf{k}_+$ and $\mathbf{k}_-$, respectively. In the case of an anisotropic superconductor, the two types of the quasiparticles experience different pair potentials (effective pair potentials),

$$\Delta_\pm=\Delta(\mathbf{k}_\pm)\equiv|\Delta_\pm|e^{i\theta_\pm}\ , \tag{1}$$

where $\theta_\pm$ are the phases of the effective pair potentials. By solving Bogoliubov-de Gennes equation, the wave function of this system can be obtained.[7,8] The reflection amplitude of holes $a(E,\varphi)$ and electrons $b(E,\varphi)$ are given by

$$a(E,\varphi)=\frac{4e^{-i\theta_+}\sqrt{E+\Omega_-}\sqrt{E-\Omega_+}}{(4+Z^2)\sqrt{E+\Omega_-}\sqrt{E+\Omega_+}-e^{i(\theta_d-\theta_++\theta_-)}Z^2\sqrt{E-\Omega_-}\sqrt{E-\Omega_+}}\ ,$$
$$b(E,\varphi)=\frac{-Z(2i+Z)[\sqrt{E+\Omega_-}\sqrt{E_+\Omega_+}-e^{i(\theta_d-\theta_++\theta_-)}\sqrt{E-\Omega_-}\sqrt{E-\Omega_+}]}{e^{2iq^+d_n}[(4+Z^2)\sqrt{E+\Omega_-}\sqrt{E+\Omega_+}-e^{i(\theta_d-\theta_++\theta_-)}Z^2\sqrt{E-\Omega_-}\sqrt{E-\Omega_+}]}\ , \tag{2}$$

where

$$\Omega_\pm=\sqrt{E^2-|\Delta_\pm|^2}\ ,\quad \theta_d=\frac{4md_nE}{\hbar^2k_F\cos\varphi}\ ,$$
$$Z=\frac{2mH}{\hbar^2k_F\cos\varphi}\ ,\quad q^+=\sqrt{k_F^2+2mE/\hbar^2}\cos\varphi\ . \tag{3}$$

Equation (2) is the generalization of Eq. (5) of Ref. 8 to include an additional N_2 layer, and reduces to it when d_n is set to zero. As is well known, the virtual bound states are formed in N_2.[9] In the case of large $Z\gg1$, the energies of the bound states determined by the divergence of the denominator of the coefficients are given as the solution of

$$\sqrt{E+\Omega_-}\sqrt{E+\Omega_+}=e^{i(\theta_d-\theta_++\theta_-)}\sqrt{E-\Omega_-}\sqrt{E-\Omega_+}\ . \tag{4}$$

The relationship between the symmetry of the pair potential and the equation giving the energy of bound states are summarized in Table I. In this table, simplification is made under the assumption of $|\Delta_+|=|\Delta_-|$ to understand the results clearly. In the case of s-wave symmetry, Eq. (4) is reduced to Eq. (a) of Table I, which is equivalent to that given by de Gennes and Saint James.[9] In the case of $d_{x^2-y^2}$-wave symmetry, the same equation as the case of the s wave holds when the c axis of S is normal to the interface (c-axis tunneling). However, in the case when the c axis is in the plane of the interface (ab-plane tunneling), the condition depends strongly on the value of φ and the axis orientation. The misorientation α in ab plane tunneling is defined by the angle between the a axis of S and the x axis. At some angle region, the signs of Δ_+ and Δ_- are reversed. In such a case, Eq. (4) is reduced to Eq. (c) of Table I, which is satisfied by $E=0$. This means the midgap states are formed just at the Fermi level. In the case of the generalized form of the pair potential, the energy level of bound states shifts from zero to a finite value depending on the phases of effective pair potentials.

The normalized conductance $\sigma(E,\varphi)$ of this system for certain angle φ is described as follows:[10–12]

$$\sigma(E,\varphi)=\frac{dI/dV}{(dI/dV)_N}=1+|a(E,\varphi)|^2-|b(E,\varphi)|^2\ , \tag{5}$$

TABLE I. The relation between the pair potential and the equation giving the energy of bound states. The equations are simplified under the assumption of $|\Delta_+|=|\Delta_-|$.

Symmetry	Effective pair potential	Equation giving the energy of bounded states	
s	$\Delta_+=\Delta_-$		(a)
$d_{x^2-y^2}$ (c-axis tunneling)	$\theta_+=\theta_-=0$	$\frac{\sqrt{\Delta_+^2-E^2}}{E}=\tan\left[\frac{2md_nE}{\hbar^2k_f\cos\varphi}\right]$	
$d_{x^2-y^2}$ (ab-axis tunneling)	$\Delta_+=\Delta_0\cos\{2(\alpha-\varphi)\}$	$\frac{\sqrt{\Delta_+^2-E^2}}{E}=\tan\left[\frac{2md_nE}{\hbar^2k_f\cos\varphi}\right]$ for $\Delta_+=\Delta_-$	(b)
	$\Delta_-=\Delta_0\cos\{2(\alpha+\varphi)\}$		
	$(\theta_+=0 \text{ or } \pi, \theta_-=0 \text{ or } \pi)$	$\frac{E}{\sqrt{\Delta_+^2-E^2}}=-\tan\left[\frac{2md_nE}{\hbar^2k_f\cos\varphi}\right]$ for $\Delta_+=-\Delta_-$	(c)
General	$\Delta_+=\lvert\Delta_+\rvert\exp(i\theta_+)$	$\frac{\sqrt{\lvert\Delta_+\rvert^2-E^2}}{E}=\tan\left[\frac{2md_nE}{\hbar^2k_f\cos\varphi}-\frac{(\theta_+-\theta_-}{2}\right]$	(d)
	$\Delta_-=\lvert\Delta_-\rvert\exp(i\theta_-)$	for $\lvert\Delta_+\rvert=\lvert\Delta_-\rvert$	

where $(dI/dV)_N$ is the tunneling conductance in the normal state. The conductance spectra have peaks at the energy level of bound states. As Z becomes larger, the conductance peak becomes higher and sharper. The experimentally observed conductance is given by the integration of $\sigma(E,\varphi)$ in the k space:

$$\sigma(eV)\propto\int_{-\infty}^{\infty}dE\int_{\Omega}d\omega\, e^{-\lambda\varphi^2}\sigma(E,\varphi)\left[\frac{-\partial f(E+eV)}{\partial E}\right], \tag{6}$$

where λ relates to the spread of tunneling electron in k space, eV is the electron energy, and $f(E)$ is the Fermi function. The value of λ depends on the form of electrode, the Fermi energy, and the work function of the barrier, and takes a value between 0–50.[13] In the case of c-axis tunneling, the integration region Ω is a three-dimensional half sphere, while in the case of ab-plane tunneling, it is a two-dimensional half circle for simplicity. Figure 3 shows the calculated spectra of PETS of the $d_{x^2-y^2}$-wave superconductor. In the case of c-axis tunneling, the spectrum has a V-shaped gap structure. In the case of ab-plane tunneling with $\alpha=\pi/4$, which corresponds to d_{xy}-wave symmetry, the ZBCP is reproduced reflecting the formation of midgap states. However, when $\alpha=0$, the gap structure with the flat bottom is reproduced. It should be noted that, in contrast to the case of the s-wave superconductors, these various types of spectra in the PETS are the peculiar features of $d_{x^2-y^2}$ wave superconductors.

There are several proposals for the origin of the ZBCP including the Anderson-Appelbaum (AA) model which assumes the existence of localized spin moments inside the tunnel barrier.[14] We think the origin of the ZBCP's is the proximity effect at the surface-degraded layers on d-wave superconductors. Our model consistently explains many features of the spectra obtained in the experiments as discussed in the following. First, all the spectra with ZBCP accompany dips just outside the peaks in the experiment. The dips cannot be explained by the AA model. Since our data were obtained by STM/S, this feature was not originated from the spatial average of gap and peak structures. Figure 4 shows the comparison of our experiment with the present model. In the figure, the experimental spectrum is normalized by the linear background conductance[15] and the parameters are taken to fit the data. It is clear that the spectrum of PETS for S having d-wave symmetry fits well the experimental spectrum. The peak height of the calculated spectrum is somewhat

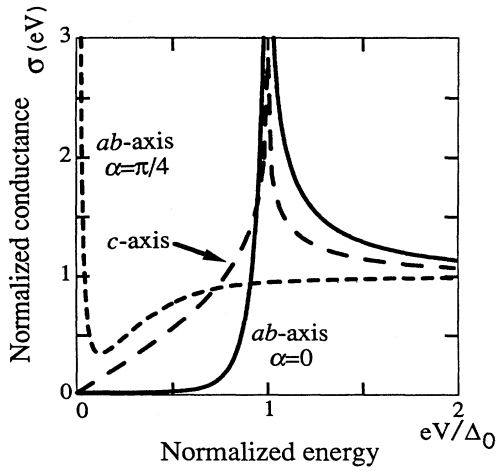

FIG. 3. Calculated tunneling spectra of PETS with S having $d_{x^2-y^2}$-wave symmetry plotted as a function of eV/Δ_0: (a) c-axis tunneling, (b) ab-plane tunneling ($\alpha=0$), and (c) ab-plane tunneling ($\alpha=\pi/4$) with $\lambda=20$, $Z=10$, $\theta_{d_{(E=\Delta_0)}}=\pi/100$, and the temperature of 0 K.

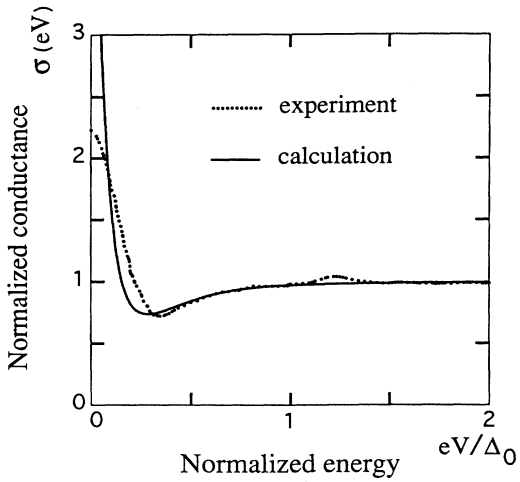

FIG. 4. Comparison of calculated spectra with experiment. Dots represent the experimental data of a YBCO(100) film in the absence of magnetic field with the bias voltage of 30 mV and the current of 1 nA. The experimental spectrum is normalized by its linear background. The line for normalization is selected to fit the conductance curve outside the gap (30–60 meV). Solid line represents the calculation with $\lambda=10$, $Z=3$, $\theta_{d_{(E=\Delta_0)}}=\pi/100$, $\alpha=\pi/4$, $\Delta_0=17.8$ meV, and the temperature of 4.2 K.

enhanced compared with that of the experiment. The agreement will be improved by taking account of the impurity scattering and the roughness of the interfaces in the calculation. Second, the midgap states form dispersionless half-filled bands and are expected to respond to the applied magnetic field as discussed by Hu.[4] The response of the ZBCP to the applied field was used for the basis of the validity of AA model. However, the ZBCP in our model also explains this feature. In the experiment, the strength of the response varies with position possibly because of the nonuniformity of the field penetration to the sample. Third, from the temperature dependence of the conductance, the ZBCP of the tunnel junctions were reported to disappear almost at the critical temperature of the superconductor.[16] This implies the strong correlation of ZBCP with pair potential and is consistent with our model. Finally, in our model, no ZBCP is predicted in *c*-axis tunneling except at the steps on the surface. This is also consistent with the experimental fact of anisotropic appearance of ZBCP depending on the film orientation. On the surface of the *a*-axis film, as seen by STM topography, misorientation is intrinsically involved. This misorientation serves as the formation of midgap states and ZBCP in the *a*-axis film. Note that a V-shaped spectrum was observed in the *c*-axis tunneling of YBCO with careful surface treatment,[17] which is the also consistent with the above calculation.

As is well known, the surfaces of the high-T_c superconductors are easily degraded. We believe that the degraded surface layer of YBCO is conductive and behaves as *N*. It is important that similar ZBCP's were widely observed on other high-T_c superconductors using tunnel junctions.[2,6] Since the ZBCP cannot be expected in the tunneling experiments of *s*-wave superconductors, it is one of the evidences that the high-T_c superconductors have *d*-wave symmetry. However, the above discussion does not reject the possibility of pair potential with more complex symmetry. As a consequence of our calculations, it is clear that the symmetry of the pair potential can be definitely determined by PETS with controlled axis orientation and *S-N* interface. By combining the PETS with LT-STM/S, we will be able to observe microscopically the spatial variation of the symmetry of the pair potential, for example, due to the spatial variation of oxygen concentration.

We would like to thank M. Matsuda for preparing the samples. One of the authors Y.T. is supported by a Grant-in-Aid for Scientific Research in Priority Areas, "Science of High-T_c Superconductivity," from the Ministry of Education of Japan.

[1]T. Hasegawa and K. Kitazawa, J. Phys. Chem. Solids **54**, 1351 (1993).
[2]T. Walsh, Int. J. Mod. Phys. B **6**, 125 (1992), and references therein.
[3]Chia-Ren Hu, Phys. Rev. Lett. **72**, 1526 (1994).
[4]S. Kashiwaya, M. Koyanagi, and A. Shoji, Appl. Phys. Lett. **61**, 1847 (1992).
[5]M. Matsuda, A. Shoji, H. Matsuhasi, and M. Koyanagi, *Advances in Superconductivity IV* (Springer-Verlag, Tokyo, 1992), p. 719.
[6]J. Lesueur *et al.*, Physica C **191**, 325 (1992), and references therein.
[7]Chr. Bruder, Phys. Rev. B **41**, 4017 (1990).
[8]Y. Tanaka and S. Kashiwaya (unpublished).
[9]P. G. de Gennes and D. Saint James, Phys. Lett. **4** 151 (1963).
[10]G. E. Blonder, M. Tinkham, and T. M. Klapwidjk, Phys. Rev. B **25**, 4515 (1982).
[11]A. Hahn, Phys. Rev. B **31**, 2816 (1985).
[12]Y. Tanaka, Phys. Rev. B **47**, 287 (1993).
[13]E. L. Wolf and G. B. Arnold, Phys. Rep. **91**, 31 (1982).
[14]J. A. Appelbaum, Phys. Rev. **154**, 633 (1967).
[15]J. R. Kirtley and D. J. Scalapino, Phys. Rev. Lett. **65**, 798 (1990).
[16]For example, see K. Hirata *et al.*, Appl. Phys. Lett. **56**, 683 (1990).
[17]H. L. Edwards, J. T. Markert, and A. J. Lozanne, Phys. Rev. Lett. **69**, 2967 (1992).